ASGE Vol. 06 (01), pp. 24-36, 2022

International Journal of Advances in Structural and Geotechnical Engineering

https://asge.journals.ekb.eg/

Print ISSN 2785-9509 *Online ISSN 2812-5142*

BEHAVIOR OF POST-OPENED DEEP BEAM RETROFITTED BY USING FERROCEMENT LAYERS.

Tarek I. Ebeido[1], Ahmed M. Tarabia[2], Yehia M. Aboziada[3]

[1]Professor, Faculty of Engineering, Alexandria University, Egypt
E-mail: ebeidotarek@yahoo.com
[2]Assoiat Professor, Faculty of Engineering, Alexandria University, Egypt
E-mail: Amtarabia@gmail.com
[3]Demonstrator, Faculty of Engineering, Alexandria University, Egypt
E-mail: Yehia.aboziadai@alexu.edu.eg

1. ABSTRACT

This paper presents an experimental program conducted on four simply supported deep beams. One of these beams was kept solid without openings as a reference beam, whereas the rest of the beams had two openings one in each shear span which opened after casting using a drilling core machine. All the tested beams were manufactured using high-strength concrete and tested up to failure under the effect of two concentrated loads one on each shear span. The main objective of these experiments is to investigate the behavior of deep beams with openings strengthened using ferrocement outer layers. The use of the shear connectors to join the ferrocement outer layers with the original beam was the main studied parameter. Beam deflection, steel strain, crack propagation, and failure modes were recorded for all the tested beams. The results have shown that the presence of openings resulted in a significant reduction in both the initial stiffness and the shear strength. Also, the retrofitting of the deep beams with ferrocement outer layers and adding shear connectors can regain the beam capacity. Finally, the presence of the shear connectors changed the failure mode of the strengthened beam from de-bonding to shear failure.

Keywords: Shear strengthening, deep beams, ferrocement layer, web openings

.

2. INTRODUCTION

Deep Beams have plenty of applications such as walls in tanks, foundations, floor diaphragms, and shear walls [1-7]. In the architecture of modern structures, transverse openings are also created through beams for the passing of service ducts, air conditions, and pipes to make better use of the other dead spaces below the beam soffit [8-12]. If the web openings intersect the load path that connects between the support and loading points, a significant reduction in the beam capacity will happen [13-15]. As a result, special reinforcement should be provided either internally or externally around the opening to limit the width of cracks to keep the beam from failure and regain the original strength of the beam. Many studies have recorded attempts to improve the ultimate capacity of deep RC beams with web openings by using different strengthening methods such as fixed-external Steel plates, the near-surface mounted bars (NSM), and bonded fiber-polymer strips sheets (FRP).

Siriluk et al. [16] investigated the efficiency of hemp fibers polymer composites in shear strengthening of deep beams. Hemp fibers are natural fibers that can be extracted from plants. Two different techniques of hemp fibers with different thicknesses were conducted in this study including two vertical sides of the beam, and three sides as U-shaped. The hemp fibers were externally fixed using an epoxy adhesive material after preparing the surface. Test results indicated that hemp fiber reinforced polymer composite was capable of enhancing. The experimental results showed that using hemp fibers as U-shaped was the best strengthening scheme. Also, the capacity of the strengthened beams was increased by 29% to 46% comparing with the control beam. Khalaf et al. [17] studied the effect of the prestressed external strands as a strengthening method on 9 deep beams with different sizes of precast rectangular openings in the shear span. Two different orientations of strands were used in this study, which were vertical, and horizontal bars. Steel plates were used to anchor the strands were placed at the end faces of beams. A hydraulic prestress jack was used for pre-stressing the external strands. It was found that the ultimate load of deep beams was increased in the horizontal strands by the range of 32–53%. On the other hand, the vertical scheme increased the beam capacity by the range of 27-33%. Rahim et al. [18] conducted a study on nine opened web deep beams strengthened using externally carbon fiber reinforced polymer strips (CFRP). The CFRP sheets were wrapped around the openings at both the tension and compression zones in one layer and up to three layers using epoxy adhesive after preparing the concrete surface. The results showed that the presence of openings in shear spans decreased the ultimate capacity by 30% when compared with the solid beams. However, the strengthening by CFRP for beams with openings regain the capacity load by 10%–40% comparing with the opened deep beam without strengthening. Chin et al. [19] presented an experimental study on 3 deep beams with circular openings strengthened by using externally bonded Carbon Fiber Reinforced Polymer (CFRP). CFRP was wrapped vertically around the openings using epoxy adhesive after preparing the concrete surface. The results showed that the presence of circular openings in shear spans decreased the ultimate capacity by 51% when compared with the solid beams. However, the strengthening by CFRP for beams with openings regain the capacity load by 15.4% comparing with the opened deep beam without strengthening.

3. Research significance:

The main purpose of this paper was to study the behavior of simply supported deep beams with openings retrofitted by the ferrocement outer layers and shear connectors.

4. METHODOLOGY:

4.1 Specimens' details:

Four RC deep beams were considered in this study, the beams were divided into a solid beam as the reference beam while the remaining three beams were with openings located at the middle of each shear span. All the openings were formed after casting using the drilling core machine described in AASHTO [20], while four small adjacents drilled cylinders with 100 mm outer diameter were drilled through the beams in each shear span and reshaped to be a square opening with dimension 200*200 as shown in Fig. 1. All the beams had an identical cross-section of 150 mm x 800 mm and an effective length of 1300 mm. The ratio of the effective length to the beam depth (Le/d) in this study was 1.25, thus the beam dimensions fulfilling the code's requirements [21-22] for deep beams.

The control beam (B1) was a concrete beam with no opening while the second beam (B2) had two symmetric square openings of dimension 200 x 200 mm, one in each shear span, and was formed after casting using the core technique. The third one (B3) is the same as the previous one but strengthened by a 50 mm ferrocement layer on both exterior sides of the beam after roughening the surface manually by hand-chiseling, whereas the next one (B4) was strengthened by adding shear connectors of diameter 12 mm to the ferrocement layers in (B3). Fig. 2 illustrates the details of all the tested beams, whereas Table. 1 summarized the strengthening techniques for the tested beams.

As for the flexure steel reinforcement, six 16 mm diameter bars were used as the bottom tension reinforcement, whereas two 16 mm diameter bars act as the compression reinforcement. For shear resistance, the side reinforcements used in both horizontal and vertical directions were 2 branches of 12 mm in diameter with a spacing of 100 mm. Fig. 3 illustrates the reinforcement details of the tested deep beams.

Table. 1: strengthening schemes of the tested beams.

Beam	Type of openings	The thickness of the ferrocement layer	Shear connectors diameter
B1 (control)	Without openings	N.A.	N.A.
B2	Two square openings (200*200) in each shear span	N.A.	N.A.
B3		50mm	N.A.
B4		50mm	12mm

N.A. not available.

Fig. 1: construction of the openings using drilling core machine.

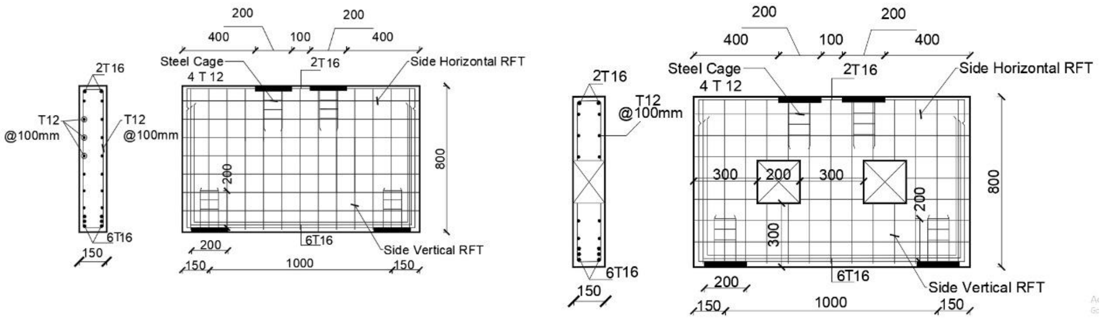

a- B1 b- B2

Fig.2: detailing of the tested beams (Note: all dimensions in mm).

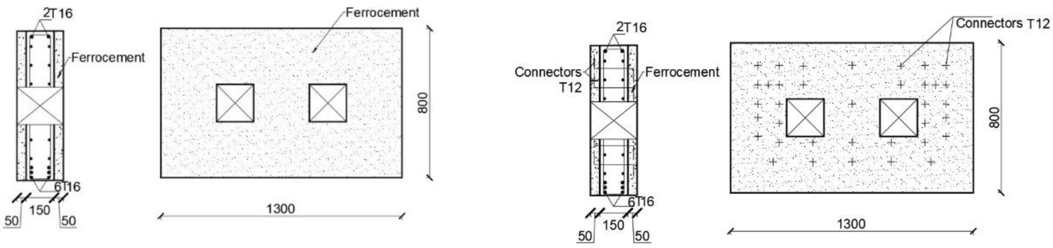

c- B3 d- B4

Fig. 2 cont: detailing of the tested beams (Note: all dimensions in mm).

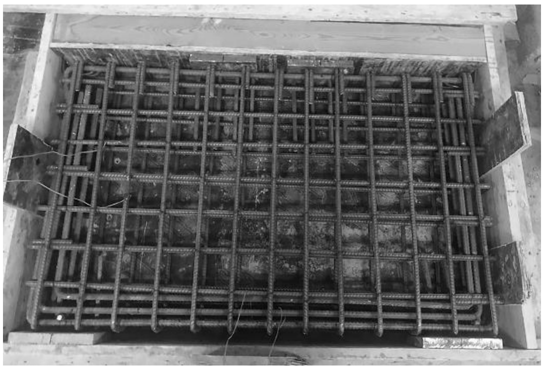

Fig. 3: reinforcements details of the tested beams.

4.2 Material characteristics:

The concrete mix and the ferrocement mortar had weight proportions shown in Table. 2. Also, Table. 3 Presents the mechanical properties of the steel reinforcement. The concrete mix consisted of ordinary Portland Cement, crushed dark basalt natural siliceous sand, and water. The Cement weight was 650 kg for each cubic meter of concrete and the nominal size of the basalt was 9.5 mm. A fine admixture (silica-fume) was used by replacing 10% of cement weight to reach the required strength. Also, the superplasticizer admixture (Master Glenium RMC 315) was used to increase the workability and fulfilling the target strength of the mix. All specimens were cured under proper conditions using wet sheets for 7 days. For the Ferrocement layer, a polypropylene fiber was added to the mortar to increase the tensile strength and reduce the microcracks. The average value of the compressive and tensile strength of the concrete mix and the ferrocement mortar were illustrated in Table. 4. To determine the tensile strength, six prisms of 100 × 100 × 500 mm were tested as shown in Fig. 4.

Table. 2: mix proportion by weight for HSC and Ferrocement mortar with respect of Cementitious material.

Mix	Cementitious material		Sand	Basalt	water bander ratio (W/b)	superplasticizer admixture
	cement	fine admixture (silica-fume)				
High strength concrete (HSC)	0.9	0.1	1.6	2.55	0.26	3% of the cementitious weight
Ferrocement	0.9	0.1	1.25	…..	0.26	3% of the cementitious weight

Table. 3: mechanical properties of steel reinforcement.

Item	Bar diammater	f_y (MPa)	f_u (MPa)
Bottom reinforcement	16 mm	560	720
Side reinforcement	12 mm	570	700

In which
(f_y): Yield stress.
(f_u): Maximum stress.

Table. 4: mechanical properties of the concrete and Ferrocement mix.

Type	Average compressive strength (MPa)	Average rapture tensile strength (MPa)
Concrete mix	After 28 days (74)	2.4
Ferrocement mix	After 21 days (64)	4.0

a- The shape of the prism.

b- Rupture test machine.

Fig. 4: determination of the tensile strength for the concrete or ferrocement mix.

4.3 Test setup:

Tests were carried out with specimens placed vertically under a 4-point load. All the test specimens were tested using a 3000 kN hydraulic machine and the load was applied with a small increment of loads equal to 50 kN. The instrumentation consisted of a loading machine, distributing girder, roller supports, and three dial gauges mounted on the longitudinal face of each specimen to measure the vertical deflection of the specimens as shown in Fig. 5. In all the tested specimens, three strain gauges were used to detect the strain of the reinforcement, each one was 10 mm in length as shown in Fig. 6.

The hydraulic machine started to push the distributing girder down with 50 kN per increment up to failure. During each load increment, cracks (if any) were marked, deflection and steel strain readings were recorded. The duration of each increment was about one minute, and the dial gauges were removed just after the failure occurred.

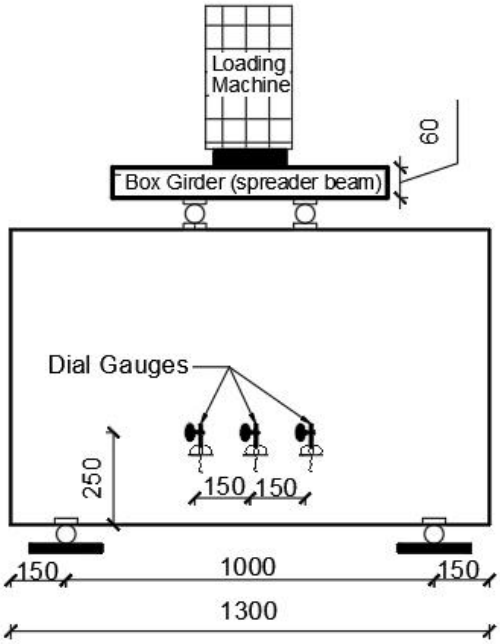

Fig. 5: test setup and position of dial gauges of the beams.

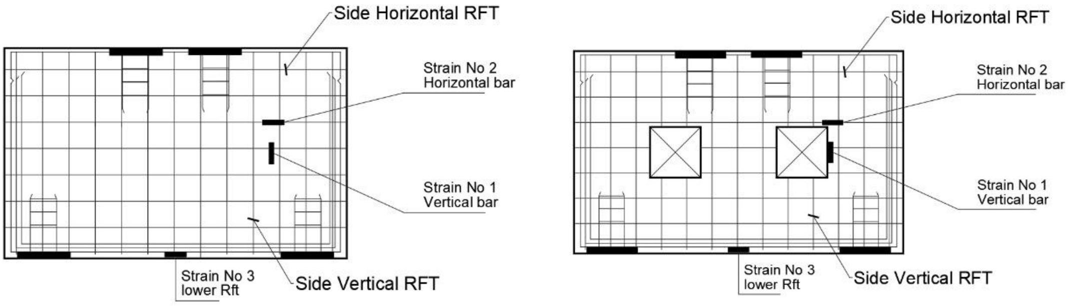

a- Strain position in the solid control beam

b- Strain positions in the beam with openings.

Fig. 6: location of strain gauges in the tested beams.

5. Experiment results

5.1 Effect of web openings

The path of loading of the vertical loads in deep beams was transported from the loading plates to the supporting plates. If the web openings interrupt the path of loading, there would be a reduction in the ultimate shear strength of the opened beams. Table. 5 shows both the first cracking (P_{crsh}) and ultimate load (P_u) for all the tested beams, whereas, Fig. 7 depicts the effect of post drilled web openings in both the cracking load and ultimate load of the control solid deep and the beam with web opening. It was found that there was a reduction in both craking load and ultimate load in B2 by 33% and 31% respectively in comparison with the solid deep beam (B1).

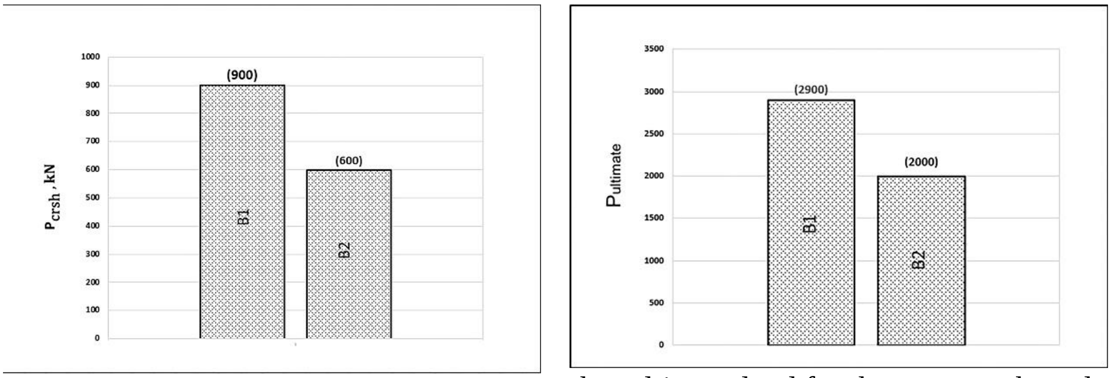

a- First cracking load for the unstrengthened beams.

b- ultimate load for the unstrengthened beams.

Fig. 7: reduction in craking load and ultimate load due to the presence of web openings.

5.2 Effect of strengthening with the ferrocement outer layers

To compensate for the reduction due to the web openings in B2, two strengthening schemes were applied in the present study. For B3 with a 50 mm ferrocement layer on both exterior sides of the beam, it was found that there was a minor improvement in the beam capacity, and the first cracking load by 2.5% and 16.6% respectively when compared with B2. On the other hand, it was recorded as a great enhancement in beam capacity and cracking load for B4 with a 50 mm ferrocement layer on both exterior sides of the beam and shear connectors by 50% and 33% respectively when compared with B2. Fig. 8 shows the effect of the strengthening techniques in the cracking load and the beam capacity in comparison with the unstrengthened beams.

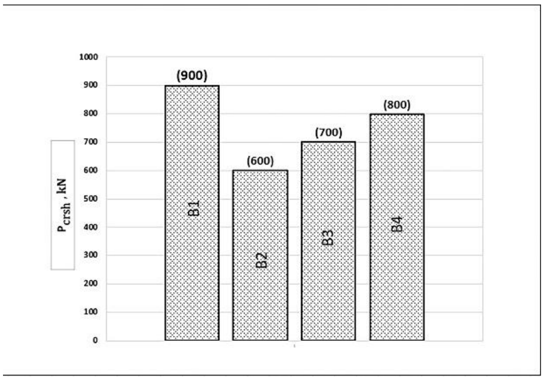

a- First craking load in the shear zone.

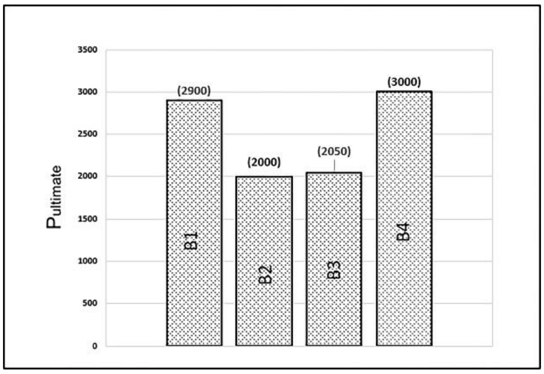

b- Ultimate load for the tested beams.

Fig. 8: comparison in first craking load and ultimate load for all the tested beams.

5.3 Craking pattern and failure modes

Fig. 9 illustrates the craking patterns of all the tested deep beams at the failure load. For the control solid beam (B1), hair cracks were observed at both the mid-span and above supports at a load of 900 kN (about 30 % of failure load, P_u), as the load was increased, the cracks gradually extended upward towards the point of loading. Just before failure, the two shear spans showed nearly identical crack patterns. The failure occurred suddenly at a load of 2900 kN in the zone above the supporting plate accompanied by the crushing of concrete. The mode of failure is classified as bearing failure.

B2 was an unstrengthened beam with two post square openings one in each shear span, firstly a set of diagonals hair cracks appeared at both the mid-span and above supports at a load of 600 kN (about 30 % of P_u). As the load was increased, these cracks gradually extended upward towards the point of loading. Just before the failure, the two shear spans showed nearly the same crack patterns. The failure occurred suddenly at a load of 2000 kN along the diagonal crack above and below the web opening extending from the loading point to the exterior end. This mode of failure may be classified as a shear failure.

For B3 with a 50 mm ferrocement layer on both exterior sides of the beam, it can be found that the first recorded cracks were vertical in the interface line between the ferrocement layer and the original beam at a load of 450 kN (about 21 % of P_u). After that, a set of diagonal hair cracks occurred above and beneath the openings at a load of 700 kN (about 35 % of P_u). As the load was raised, the cracks gradually extended towards the opening and loading plates. The failure occurred suddenly at a load of 2050 kN due to the delaminating and debonding of the ferrocement layers from the beam which can be classified as the failure of debonding.
B4 was strengthened with shear connectors of 12 mm diameter to connect the ferrocement layers to the original beam. Diagonal hair cracks were found at a load of 800 kN (about 26% of P_u) above the supporting plates in shear zones. The diagonal cracks became wide and intense as the load increased, then these cracks enlarged and reached the loading plates. A sudden failure occurred at a load of 3000 kN along the

diagonal cracks extending above and below the corner of the opening. This mode of failure can be classified as a shear failure

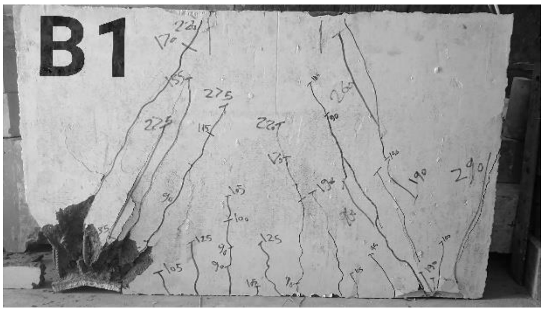

a- Cracking patterns of B1 after failure

b- Bearing failure of B1

a- Cracking patterns of B2after failure

b- The back longitudinal side of B2

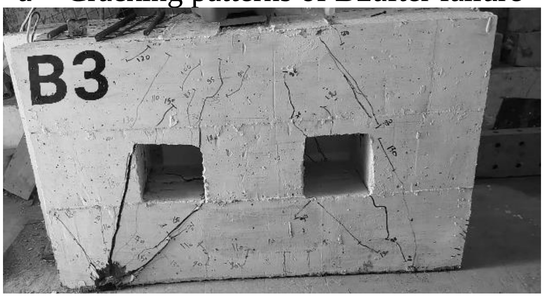

a- Cracking patterns of B3 after failure

b- Side view of B3

Fig.9: crack patterns of all tested beams at failure load.

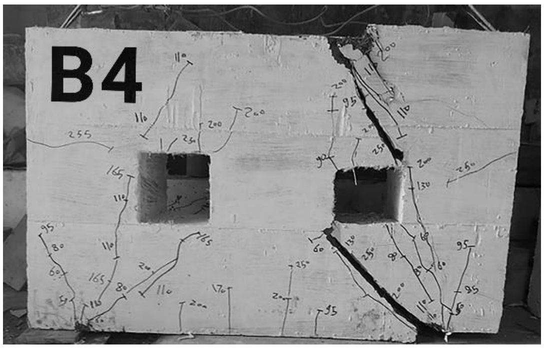

a- Cracking patterns of B4 after failure

b- Side view of B4

Fig. 9 cont: crack patterns of all tested beams at failure load.

5.4 Load deflection curves

Three dial gauges were mounted on the longitudinal face of each specimen to measure the vertical deflection of the tested beam at every load increment. Table. 5 shows the values of mid-span deflection at both the yielding load of the bottom longitudinal bar (P_y) and the ultimate load (P_u). Also, Fig. 10 shows the load-midspan deflection for all the tested beams. It can be found that the maximum deflection of B1 was smaller than B2 about 8.7%. The maximum deflection of the strengthened specimens for B3 and B4 were 7.76 and 6.71 mm respectively, which confirmed the significant usage of the shear connectors

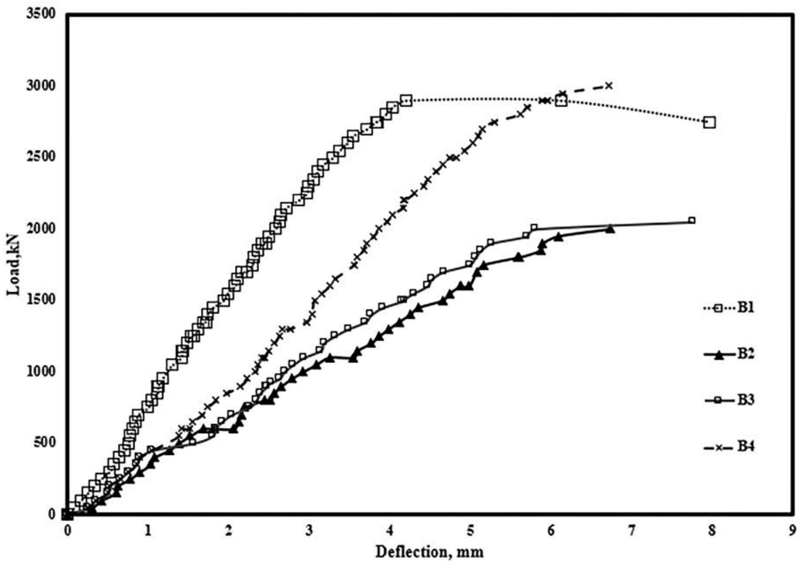

Fig. 10: load versus deflections for all the tested beams.

5.5 Stiffness and ductility

Ductility is defined as the ability of deep beams to undergo considerable deflection before the failure. To evaluate the beam ductility, the area under the load-deflection curve was calculated. Also, the slope of the load-deflection curve for each beam was calculated to assess the stiffness of the tested deep beam. Table. 5 illustrates the values of both stiffness and ductility for all the tested beams. It was found that the reduction in the beam stiffness and ductility was about 58.4 % and 57.8% respectively as the presence of web openings in the shear span. On the other hand, strengthening the beam with ferrocement layers only improved the beam stiffness and ductility by 2% and 37.5% respectively when compared with the unstrengthened beam with openings (B2). However, adding shear connectors to the ferrocement layers increased the beam stiffness and ductility by 26% and 33% respectively when compared with the unstrengthened beam with openings (B2).

5.6 Rebar strain

The load-rebar strain relationship in the side reinforcement and the bottom longitudinal bars for all tested beams were shown in Fig. 11. It is worth mentioning that the strain on both the vertical side reinforcement of B4 and the horizontal side reinforcement of B3 could not be measured as the malfunction of strain gauges. Table. 5 reviles the yielding load values for the bottom longitudinal bar (P_y) for all tested beams. It can be found that the yielding load in the bottom bar of B2 was smaller than B1 about 24%, this reduction due to the effect of the web openings. The yield load of the bottom reinforcement for B1 and B2 were 2500 kN and 1900 kN respectively. However, there was no yield recorded in the bottom bars for B3, as well, the yield load for B4 was 2900kN. Finally, no yielding occurred at both horizontal and vertical side reinforcements for B2 and B3.

Table. 5: exprimental results.

Specimens	Cracking load (kN)	Yield load (kN)	Ultimate load (kN)	Deflection (mm)		(Δ_u/Δ_y)	Mode of failure	$A_{p\text{-}\delta}$ (KN.m)	K (kN/mm)
	P_{crsh}	P_y	P_u	Δ_y	Δ_u				
B1	900	2500	2900	3.29	6.15	1.86	Bearing failure	17.45	803
B2	600	1850	2000	5.87	6.74	1.14	Shear failure	7.36	333.3
B3	700	NY	2050	NY	7.76	……_	Debonding of ferrocement and shear failure	10.12	340
B4	800	2800	3000	5.61	6.71	1.19	Shear failure	11	420

In which
(P_u) is the ultimate beam load.
(P_{crsh}) is the first shear cracking load.
(P_y) is the yielding load of the bottom longitudinal steel.
(Δ_y) is the deflection at mid-span at P_y
(Δ_u) is the deflection at mid-span at Pu
$(A_{p\text{-}\delta})$ is the area under the load-deflection curve (Kn.m)
(K) is the initial stiffness at 30% of the failure load (kN/mm)
(NY) no yield.

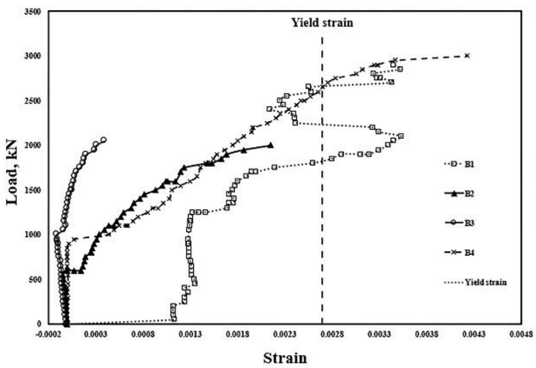

a- Load – rebar strain curve for the side horizontal reinforcement.

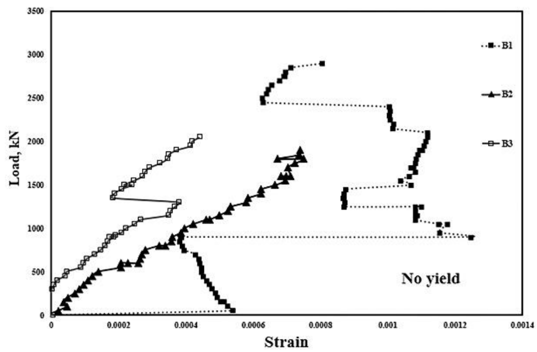

b- Load – rebar strain curve for the side vertical reinforcement.

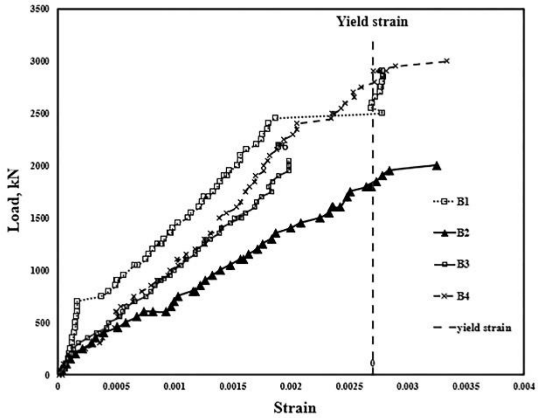

c- Load – rebar strain curve for the bottom reinforcement.

Fig. 11: load versus strain for all the tested beams.

6. CONCLUSIONS

An experimental program was conducted to investigate the behavior of RC deep beams with post-drilled web openings in the shear span strengthened by using the ferrocement outer layers. The loss in the beam capacity of the beam with openings (B2) was in the range of 31 % when compared with that of the control beam (B1). Surface strengthening using the ferrocement outer layers could increase the ultimate load capacity by 2.5% in the case without shear connectors and 50% when shear connectors were included comparing with the un-strengthened beam with openings (B2).

7. REFERENCE

[1] Mohamed, A.R., Shoukry, M.S. and Saeed, J.M., (2014). Prediction of the behavior of reinforced concrete deep beams with web openings using the finite element method. *Alexandria Engineering Journal*, *53*(2).

[2] Lee, H.K., Cheong, S.H., Ha, S.K. and Lee, C.G., (2011). Behavior and performance of RC T-section deep beams externally strengthened in shear with CFRP sheets. *Composite Structures*, *93*(2), pp.911-922.

[3] Eslam, M.R., Mansur, M.A. and Maalej, M., (2005). Shear strengthening of RC deep beams using externally bonded FRP systems. *Cement and Concrete Composites*, *27*(3), pp.413-420.

[4] Tan, K.H., Kong, F.K., Teng, S. and Guan, L., (1995). High-strength concrete deep beams with effective span and shear span variations. *Structural Journal*, *92*(4), pp.395-405.

[5] El Maaddawy, T. and Sherif, S., (2009). FRP composites for shear strengthening of reinforced concrete deep beams with openings. *Composite Structures*, *89*(1), pp.60-69.

[6] Hussain, Q. and Pimanmas, A., (2015). Shear strengthening of RC deep beams with openings using sprayed glass fiber reinforced polymer composites (SGFRP): part 1. experimental study. *KSCE Journal of civil engineering*, *19*(7), pp.2121-2133.

[7] Abduljalil, B.S., (2014). Shear resistance of reinforced concrete deep beams with opening strengthened by CFRP strips. *Journal of Engineering and Development*, *18*(1), pp.14-32.

[8] Pimanmas, A., (2010). Strengthening R/C beams with opening by externally installed FRP rods: Behavior and analysis. *Composite Structures*, *92*(8), pp.1957-1976.

[9] Sahoo, D.R., and Chao, S.H., (2010). Use of steel fiber reinforced concrete for enhanced performance of deep beams with large openings. In *Structures Congress 2010* (pp. 1981-1990).

[10] Yang, K.H., Eun, H.C. and Chung, H.S., (2006). The influence of web openings on the structural behavior of reinforced high-strength concrete deep beams. *Engineering Structures*, *28*(13), pp.1825-1834.

[11] Campione, G. and Minafò, G., (2012). The behavior of concrete deep beams with openings and low shear span-to-depth ratio. *Engineering Structures*, *41*, pp.294-306.

[12] Kumari, A. and Nayak, A.N., (2020). An experimental approach for the strengthening of RC deep beams with web openings using GFRP fabrics and gas actuated fasteners. *Journal of Building Engineering*, p.102027.

[13] Shanmugam, N.E. and Swaddiwudhipong, S., (1988). Strength of fiber reinforced concrete deep beams containing openings. *International Journal of Cement Composites and Lightweight Concrete*, *10*(1), pp.53-60.

[14] Mansur, M.A. and Alwis, W.A.M., (1984). Reinforced fiber concrete deep beams with web openings. *International Journal of Cement Composites and Lightweight Concrete*, *6*(4), pp.263-271.

[15] Hu, O.E., Tan, K.H. and Liu, X.H., (2007). Behavior and strut-and-tie predictions of high-strength concrete deep beams with trapezoidal web openings. *Magazine of Concrete Research*, *59*(7), pp.529-541.

[16] Siriluk, S., Hussin, Q., Rattanapitikorn, W. and Pimanmas, A., (2018). Behaviors Of RC deep beams strengthened in shear using hemp fiber reinforced polymer composites. *International Journal*, *15*(47), pp.89-94.

[17] Khalaf, M.R. and Al-Ahmed, A.H.A., (2020), December. Shear strength of reinforced concrete deep beams with large openings strengthened by externally prestressed strands. In *Structures* (Vol. 28, pp. 1060-1076). Elsevier.

[18] Rahim, N.I., Mohammed, B.S., Al-Fakih, A., Wahab, M.M.A., Liew, M.S., Anwar, A., and Amran, Y.H., (2020). Strengthening the Structural Behavior of Web Openings in RC Deep Beam Using CFRP. *Materials*, *13*(12), p.2804.

[19] Chin, S.C., Yahaya, F.M., Ing, D.S., Kusbiantoro, A. and Chong, W.K., (2015), September. Experimental study on shear strengthening of RC deep beams with large openings using CFRP. In *International Conference on Architecture, Structure and Civil Engineering, Antalya*.

[20] AASHTO, S. (1999). ASTM C 42/C 42M-99 Standard Test Method for Obtaining and Testing Drilled Cores and Sawed Beams of Concrete: AASHTO.

[21] ACI318M-14. (2015). *Metric Building Code Requirements for Structural Concrete & Commentary*.

[22] ECP-203. (2018). ECP-203: 20018-Egyptian Code for design and construction of concrete structures. *HBRC, Giza*.